NUCL SCI TECH (2021) 32:76
https://doi.org/10.1007/s41365-021-00907-w

Design of real-time feedback control of vertical growth rate on EAST

Na-Na Bao[1,2,3] · Yao Huang[2] · Bing-Jia Xiao[2] · Qi-Ping Yuan[2] · Zheng-Ping Luo[2] · Yue-Hang Wang[2] · Shu-Liang Chen[2]

Received: 27 January 2021 / Revised: 7 May 2021 / Accepted: 8 May 2021 / Published online: 22 July 2021

Abstract Real-time feedback control of vertical growth rate, called gamma control, has been successfully applied to experimental advanced superconducting tokamak (EAST). In this paper, a new gamma control method is proposed to regulate the vertical growth rate, which is an estimator of plasma vertical instability. Thus, the gamma controller can be utilized to keep the tokamak plasma away from its unstable boundary. In this work, the main development process includes three steps: (1) real-time implementation of model-based vertical growth rate calculation, taking advantage of GPU parallel computing capability, (2) design of plasma shape response for dynamic shape control using a slight modification to the plasma boundary, and (3) development of a gamma control algorithm integrated into the EAST plasma control system (PCS). The gamma control was experimentally verified in the EAST 2019 experiment campaign. It is shown that the time evolution of the real-time vertical growth rate agrees with the target value, indicating that the real-time vertical growth rate can be regulated by gamma control.

Keywords Experimental advanced superconducting tokamak (EAST) · Dynamic shape response · Gamma control · Vertical growth rate

✉ Yao Huang
yaohuang@ipp.ac.cn

1 School of Internet, Anhui University, Hefei 230039, China

2 Institute of Plasma Physics, Chinese Academy of Sciences, Hefei 230031, China

3 National Engineering Research Center for Agro-Ecological Big Data Analysis & Application, Anhui University, Hefei 230039, China

1 Introduction

A vertically elongated plasma cross section has been utilized to improve the performance and confinement of tokamaks. However, this causes inherent vertical instability. Because plasma vertical instability is a significant safety issue for current tokamak operations, a variety of advanced magnetic control approaches have been employed for unstable vertically elongated plasma on several tokamaks, such as JET [1], DIII-D [2], KSTAR [3], and EAST [4]. Numerical vertical control strategies have been implemented on EAST [5–7]; however, research results [8] indicate that losing control of the plasma vertical instability might be caused by various factors (such as large vertical displacement, external disturbances, and noise). The subsequent ineffectiveness at suppressing the growth rate of plasma vertical instability can lead to a vertical displacement event (VDE) and disruptions, causing considerable damage to tokamak devices [9–11]. Steady-state discharge operation requires the plasma to be continuously away from its vertically unstable boundary. Because the vertical instability of plasma strongly depends on the vertical growth rate (γ) as a critical plasma parameter [12–14], a novel feedback control strategy can be designed for real-time control of the vertical growth rate. We utilized the linear rigid plasma response model of TokSys [15] to develop a comprehensive evaluation of the vertical growth rate [16, 17]. This work is based on two important tools: a simplified equivalent axisymmetric structure model of EAST [18–20] and GPU parallel equilibrium reconstruction code, PEFIT [21–24]. In this study, the above GPU-based calculation of γ is integrated into the EAST PCS [25–28] to conduct real-time implementation. A linearly simplified model of real-time plasma shape variation with γ

during the EAST history experiments is proposed; this model can be utilized as a plasma shape response method, which cooperates with existing plasma isoflux shape control as an "actuator" for gamma control. This gamma controller follows a generic proportional–integral–derivative (PID) control law to implement closed-loop control. The gamma control algorithm is developed in the EAST PCS. The gamma controller has been preliminarily applied to EAST experiments under an upper-single null (USN) configuration because the upper divertor (made of tungsten) is more tolerant to heat loads than the lower divertor (made of graphite) in EAST. A good agreement between the real-time vertical growth rates and their corresponding target values indicates the effectiveness of the proposed gamma control method.

The remainder of this paper is organized as follows. The real-time implementation of the plasma vertical growth rate calculation is briefly described in Sect. 2. In Sect. 3, a shape response method based on an experimental result analysis is presented to investigate the dynamic plasma shape effect on the evolution of the real-time vertical growth rate. In Sect. 4, the gamma control algorithm in EAST PCS, using real-time vertical growth rate, shape response model, and PID control law, is presented. In Sect. 5, the experimental results of gamma control are presented. Finally, a summary and discussion are presented in Sect. 6.

2 Real-time implementation of calculation of γ

Real-time implementation of vertical growth rate calculation is the basis of our work. Owing to the parallel computing capabilities of a server equipped with a multi-core CPU and GPU, the calculation principle of vertical growth rate can be quickly conducted using C and CUDA C languages, taking advantage of the rigid modeling principle of the EAST vertical response system; this vertical response system model is built using fast plasma equilibrium data (such as plasma current distribution) reconstructed by PEFIT, which is a GPU parallel equilibrium reconstruction code [21–24], and the static passive EAST structural model considering the effects of three-dimensional conductors. This paper focuses implementing the γ calculation in real time, rather than the detailed calculation process (for interested readers, a more detailed introduction to the calculation of γ can be found in Refs [16, 17]).

To conduct this real-time implementation, the GPU-based host must be capable of communicating with the EAST PCS during plasma discharge. For this purpose, a reflection memory card is installed in the GPU-based host (i.e., an RT-GPU computing system) to support real-time data transmission. The data interface between this RT-GPU computing system and the EAST PCS is shown in Fig. 1. First, the EAST PCS sends shot numbers to the RT-GPU computing system. After receiving this message, data memories and 2D EAST structural data can be allocated and loaded into the computing system. Next, PEFIT reconstructs the plasma equilibrium using magnetic diagnostic data to generate the plasma current density profile and coil currents. Accordingly, the rigid plasma response variables, comprising the input matrix of the EAST vertical response model, can be calculated. Finally, the only positive eigenvalue of the input matrix, representing real-time γ, can be determined and sent to the EAST PCS. The time required for real-time data transmission can be ignored, compared with the time required to compute the vertical growth rate. In summary, the time required to implement this comprehensive calculation of γ is approximately 2 ms.

3 Model of plasma shape response

Although much attention has been given to plasma vertical control using inner vessel coils, almost no control method is available regarding shape control using poloidal coils of the present tokamak devices. Therefore, a novel shape control method is developed to keep the plasma away from its unstable boundary with regard to the real-time vertical growth rate. The model of the plasma shape response to changes in the vertical growth rate is a key part of our work. A linear model for comprehensive evaluation of the plasma shape response is established based on the EAST experiment results. The design process is described in this section.

3.1 Experimental results

In this section, we explore the relationship between the plasma shape response and vertical growth rate experimentally using the ISOFLUX/PEFIT shape control method. Specifically, the δr_{sep} control method of shape control [29] was utilized to investigate the relationship between the continuous evolution of the plasma shape and the change in γ. δr_{sep} represents the radial distance, measured at the outboard midplane between two flux surfaces where the upper and lower X-points ($X1$ and $X2$, respectively) lie, that is, $\delta r_{\mathrm{sep}} = (\psi_{X1} - \psi_{X2})/G_{\mathrm{mp}}$, where ψ is the flux value and G_{mp} is the radial flux gradient at the outboard midplane control points. Plasma boundaries change continuously when δr_{sep} is required to vary in a single shot. Our experiments were performed by varying δr_{sep} linearly with time to observe the evolution of real-time γ.

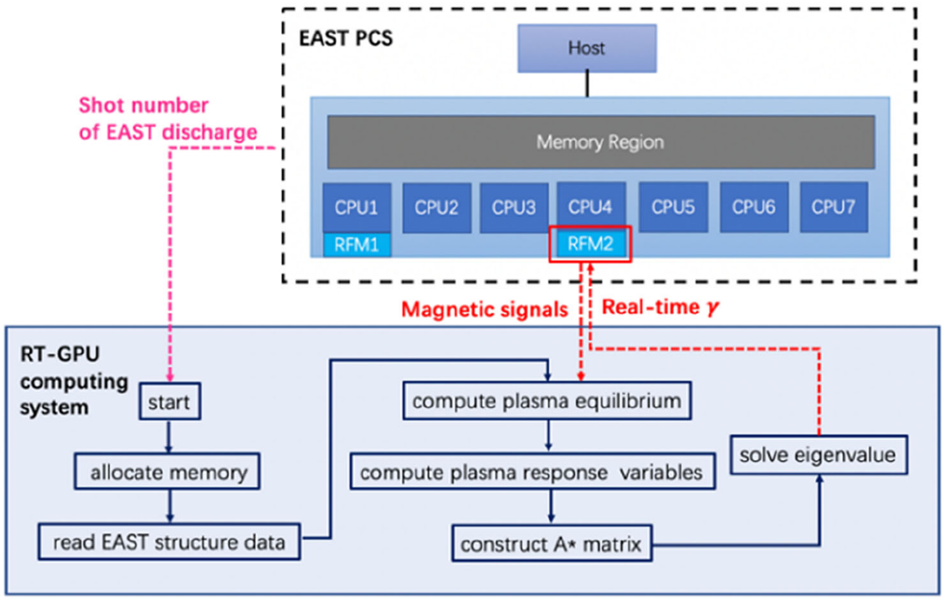

Fig. 1 (Color online) The computation flow of real-time γ and data interface between RT-GPU computing system and EAST PCS. This computing system is equipped with an NVIDIA V100 card supporting parallel computing, and an RFM card providing data transmission with EAST PCS by joining its RFM internet. The red dashed lines indicate that the RT-GPU computing system can receive magnetic diagnostic signals from PCS and send real-time values of γ to it. The pink dashed line shows that PCS can send start-up signal of discharge using the Linux Socket technology, triggering γ calculation

A δr_{sep} control experiment is shown in Fig. 2. During this discharge (EAST shot number #89485), the value of the control parameter, that is, δr_{sep}, increased from 2 to 4 cm during the interval 4–5 s. The results show that the plasma parameters—i.e., vertical position (Z), vertical growth rate (γ), and elongation (κ)—change accordingly. The upward vertical displacement, decrements of real-time γ, and plasma elongation are approximately 0.3 cm (from 0.48 to 0.78 cm), 20 s^{-1} (from 88 to 68 s^{-1}), and 0.05 (from 1.63 to 1.58), respectively, during the interval 4–5 s (refer to 1st–3rd panels in Fig. 2).

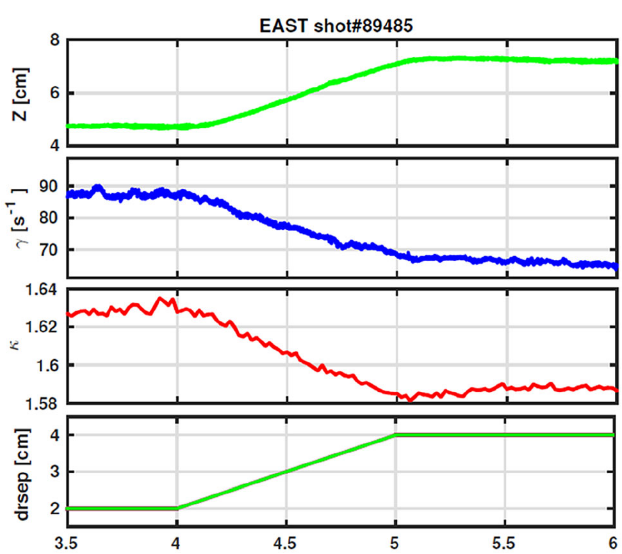

Fig. 2 (Color online) Evolution of main plasma parameters during pulse #89485. Plasma parameters in the 1st–4th panels are vertical position of plasma current center, real-time vertical growth rate, elongation, and δr_{sep}, from top to bottom

In this experiment, the plasma shape also changed. The variations in plasma shape are plotted in Fig. 3, where the reconstructed plasma shapes at different times are indicated by curves with different colors. The boundary of the vacuum vessel of the EAST tokamak is represented by a black line, and the deep purple control segments are denoted by different numbers (4, 6, 8, 3, 14, and 9). Six segments intersect with the plasma boundary in the USN discharge configuration. The position variations of these control points are different. It can be observed that the plasma shape changes continuously and the positions of control points 8 and 9 vary more dramatically than the other control points. It is shown that there is a strong dependence of the plasma shape change on the positions of control points 8 and 9, while the positions of control points 3, 4, 6, and 14 are approximately unchanged. The absolute values of the position change of control points 8 and 9 are listed in Table 1. It is obvious that the absolute values of these two control point positions are similar, but the directions of movement are different. Control point 8 moves inward, whereas control point 9 moves in the opposite direction.

Experiments using δr_{sep} control were successfully conducted. The results show that changes in the vertical growth rate strongly depend on the plasma shape and the variation in the plasma shape can be simply represented by two controlled variables, that is, the positions of control points 8 and 9.

3.2 A model of the plasma shape response

A simple model of the plasma shape response to the change in the vertical growth rate is obtained from the above experimental results. In this study, the linear fitting

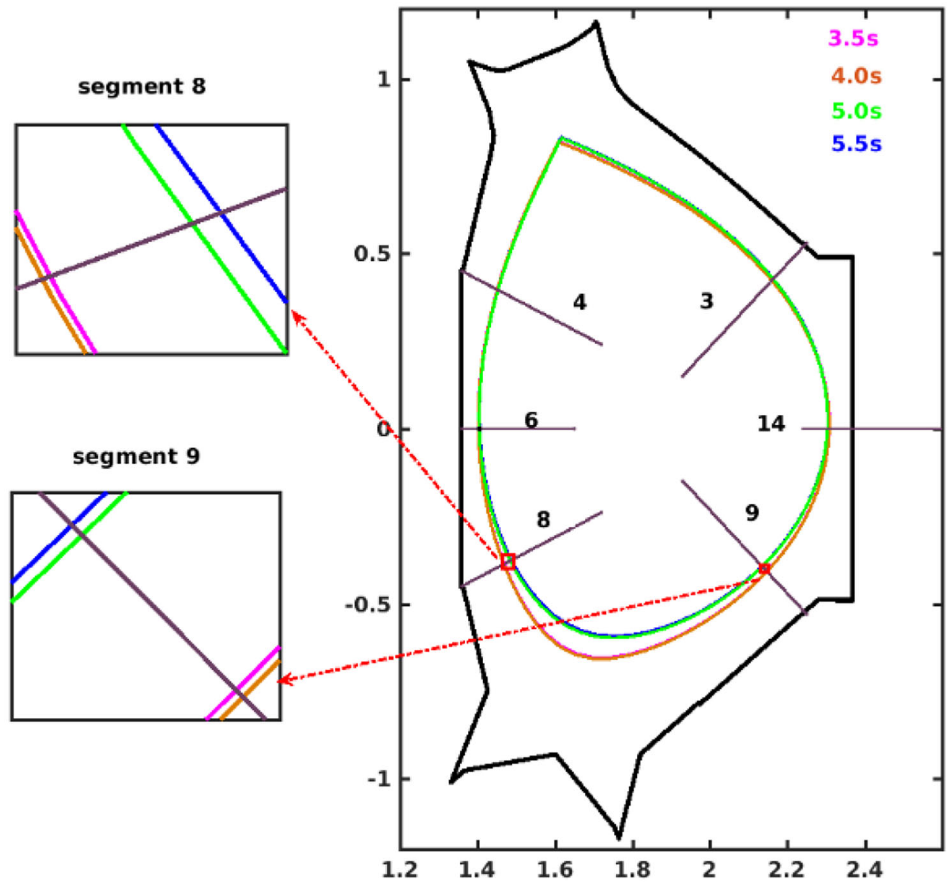

Fig. 3 (Color online) Reconstructed plasma shapes at 3.5 s (rose red line), 4 s (deep yellow line), 5 s (green line), and 5.5 s (dark blue line) during pulse #89485. The control points (8 & 9) are locally magnified in the left subfigures

Table 1 Position changes of points 8 and 9

Time (s)	3	4	5	5.5
Point 8 (mm)	0	0.1	21.8	18.2
Point 9 (mm)	0	0.8	18.9	17.8

method was used to construct an approximate shape response model. The absolute values of the control point positions are plotted with the evolution of the vertical growth rates in Fig. 4.

It is shown that the relation between real-time γ and position changes of control points 8 and 9 can be approximated with this linear function, that is,$y = -0.0012x + 0.11$, where x and y denote variations of real-time γ and positions of control points 8 or 9. The minus sign indicates that the value of the position change increases with a decrease in γ. This approximation is consistent with the data in Table 1. For example, according to the fitting function, a change of 20 s^{-1} in real-time γ corresponds to a position change of 24 mm for both control points 8 and 9, while the actual position changes are

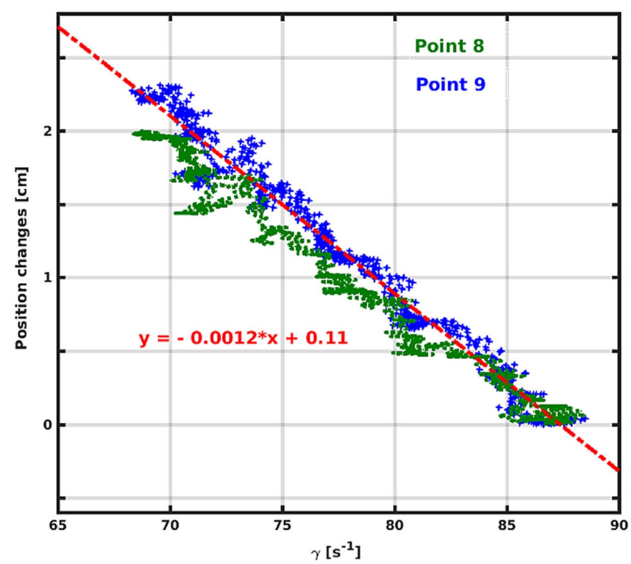

Fig. 4 (Color online) Relationship between real-time γ and position changes of control points 8 and 9. The green, blue, and red lines indicate segment 8, segment 9, and the fitting function, respectively

21.7 mm and 18.1 mm, respectively. For simplicity, the position changes of the control points (8 and 9) are considered to be the same. The shape response with limitations can be divided into the following piecewise function:

$$\Delta d = K \times \gamma_{\max}; |\gamma_{\text{error}}| > \gamma_{\max},$$

$$\Delta d = K \times \gamma_{\text{error}}; 0 < |\gamma_{\text{error}}| < \gamma_{\max},$$

where γ_{error} is the difference value obtained by subtracting the target value of γ from its real-time value, Δd represents the position change of the control point, and $\gamma_{\max}$ denotes the maximum value of the controlled γ. In this work, the value of K is preliminarily chosen as 0.15 cm · s. In practical applications, a decrease in γ is achieved by adjusting various control parameters and positions of control points 8 and 9. It is evident that the value of K can be different from the linear fitting value and should be evaluated through experiments.

4 Gamma control

In this section, the design process of gamma control for decreasing the vertical growth rate using the proposed shape response is illustrated. The gamma control method was designed following an appropriate control law. PID control is a generic feedback control law that attempts to minimize the error between a measured variable and its target value through corrective action. In our design, a typical PID controller was utilized for continuous shape changes. The PID controller has a standard relation, that is,

$$u(t) = K_{\text{p}}\left(e(t) + {}^{1}/_{T_{\text{i}}}\int_0^t e(\tau)\mathrm{d}\tau + T_{\text{d}}\mathrm{d}e(t)/\mathrm{d}t\right),$$

where $e(t) = r(t) - y(t)$, $r(t)$, and $y(t)$ are the desired and real-time values of the vertical growth rate, respectively, T_{i} and T_{d} are the time constants of the integral and derivative terms, respectively. In this form, K_{p}, $K_{\text{p}}/T_{\text{i}}$, and $K_{\text{p}}T_{\text{d}}$ denote the proportional, integral, and derivative coefficients, respectively.

Gamma control is developed under the software environment of the EAST plasma control system (PCS) as EAST PCS provides significant flexibility and control methods over EAST devices for experiment operators and control algorithm developers. For example, the plasma shape control [6] mentioned in Sect. 3 is one of the most important control methods in EAST PCS. Taking advantage of experimental results using δr_{sep} shape control, this shape response was also designed as a part of the shape control. Thus, gamma control can be considered as an augmentation to shape control in the EAST PCS. A simplified block diagram of the gamma control, cooperating with other main parts of this shape control, is shown in Fig. 5.

The designed gamma control can perform the following operations according to the experimental procedures during a discharge:

Before this discharge begins, the parameters of gamma control (such as target vertical growth rate, PID controller parameters, K coefficient) and other parameters of different control methods are defined by the experimental operators.

During discharge, the plasma is controlled by various control methods in the EAST PCS. In this paper, we only describe the gamma control and its relevant control methods. The real-time vertical growth rate is calculated on an RT-computing system and sent to the EAST PCS. Next, a dynamic boundary response to real-time γ is conducted as follows: the error of γ is generated by subtracting real-time γ from the target γ, and the desired position change value of control points (8 and 9) can be computed by multiplying the error by K coefficient to obtain the value of Δd and send Δd to its PID module. Then, a new target plasma shape is generated by changing the positions of control points 8 and 9 (i.e., the dynamical boundary response), based on the original target plasma shape set before this discharge. Finally, the real-time plasma shape can be controlled by the surrounding coils following the original plasma shape control methods [6]. The detailed process is that this new target plasma shape is compared with real-time plasma shape to calculate a set of errors, including flux errors of control points and position errors of X-points, which are then processed by the PID module and multiplied by a so-called M matrix to calculate the required poloidal field (PF) coil currents. PF coil currents should be provided by the shape control (IPFref1), plasma current control (IPFref2), slow part of vertical control (IPFref3), and feedforward setting (IFF). The error of the PF coil current can be obtained (error = IPFref1 + IPFref2 + IPFref3 + IFF − IPF), which is utilized by the PF coil current feedback control to determine the voltage commands for the power supply (PS) of the PF coils. After the discharge, the evolutions of the plasma parameters are stored for further experimental analysis.

5 Gamma control experiments

Gamma control experiments were performed during the 2019 EAST campaign to demonstrate the performance of the gamma controller. In this section, experimental results are presented to test and evaluate the effectiveness of the gamma control.

To begin this, a series of experiments were conducted using gamma control to determine an appropriate value for coefficient K. As mentioned in Sect. 3.2, because the fitted linear coefficient may not represent the actual relationship between the quantities, the value of coefficient K needs to

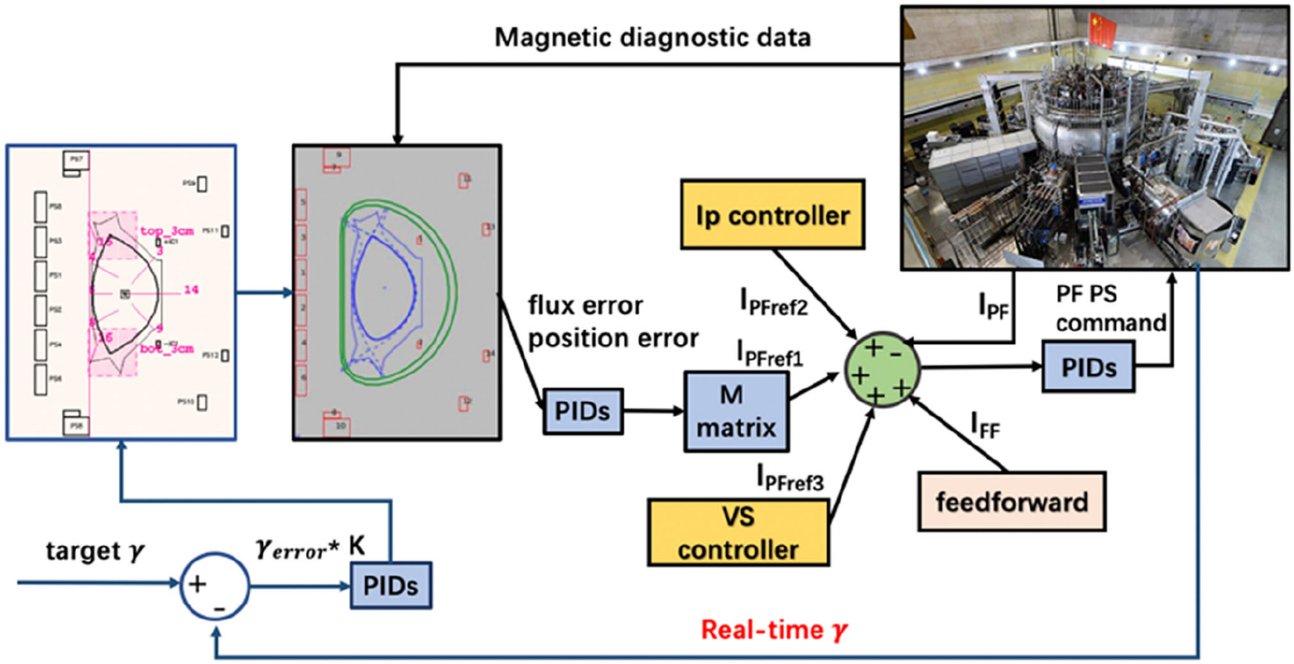

Fig. 5 (Color online) Simplified block diagram of gamma control, cooperating with plasma current control (Ip controller) and vertical position control (VS controller)

be determined through tests. The experimental results using different K values (i.e., 0.15, 0.2, and 0.25) are given in Table 2, where $\Delta target$ represents the desired change in the vertical growth rate, i.e., 20 s^{-1} in these cases and $\Delta real$ is the measured change in the vertical growth rate. These experiments were successfully conducted, demonstrating the availability of this control method and the effectiveness of gamma control with different values of coefficient K. Moreover, it can be seen that when coefficient K is 0.25, $\Delta real$ is the closest to $\Delta target$, and the best performance can be attained in terms of the experiments that have been performed on EAST. In the following experiments, the value of K was set to 0.25.

In addition to performing experiments to find a suitable K value, we also conducted a series of experiments to test different ways of changing the vertical growth rate. As shown in Fig. 6, EAST discharge #91118 was considered as the reference shot. The detailed experimental operations are as follows: (1) In the first experiment (discharge #91130), the target value of γ was kept constant at 90 s^{-1} in the time interval from 4 to 8 s. It is noteworthy that γ value of 90 s^{-1} is the real-time value of γ at 4 s during the reference shot (discharge #91118); (2) In the second experiment (discharge #91131), the target value of γ was reduced to 70 s^{-1} from 4 to 5 s and was kept constant at 70 s^{-1} from 5 to 8 s.

Table 2 Experiment results for different K coefficients

Shot number	91120	91123	91129
K coefficient	0.15	0.2	0.25
$\Delta real/\Delta target$	0.56	0.6	0.85

In Fig. 6, the evolution of the target γ is represented by the red lines, where subfigures (a) and (b) correspond to operations (1) and (2), respectively. It is shown that the time evolutions of real-time γ are both close to the target values, plotted by the green lines. Compared with the results in the reference shot plotted by the dark-blue lines, the vertical growth rates changed significantly. In the first experiment (see Fig. 6a), the elongation gradually decreased and the plasma cross section remained almost the same. In the second experiment (see Fig. 6b), the area of the plasma cross section significantly reduced during the interval 4–5 s but remained approximately unchanged after that.

It can be seen that the real-time γ can follow its target value well in both experiments, demonstrating the effectiveness of gamma control. As far as the experiment is concerned, the results are preliminary and that there is room for further optimization, such as choosing decent values for the K coefficient and PID parameters via experiments.

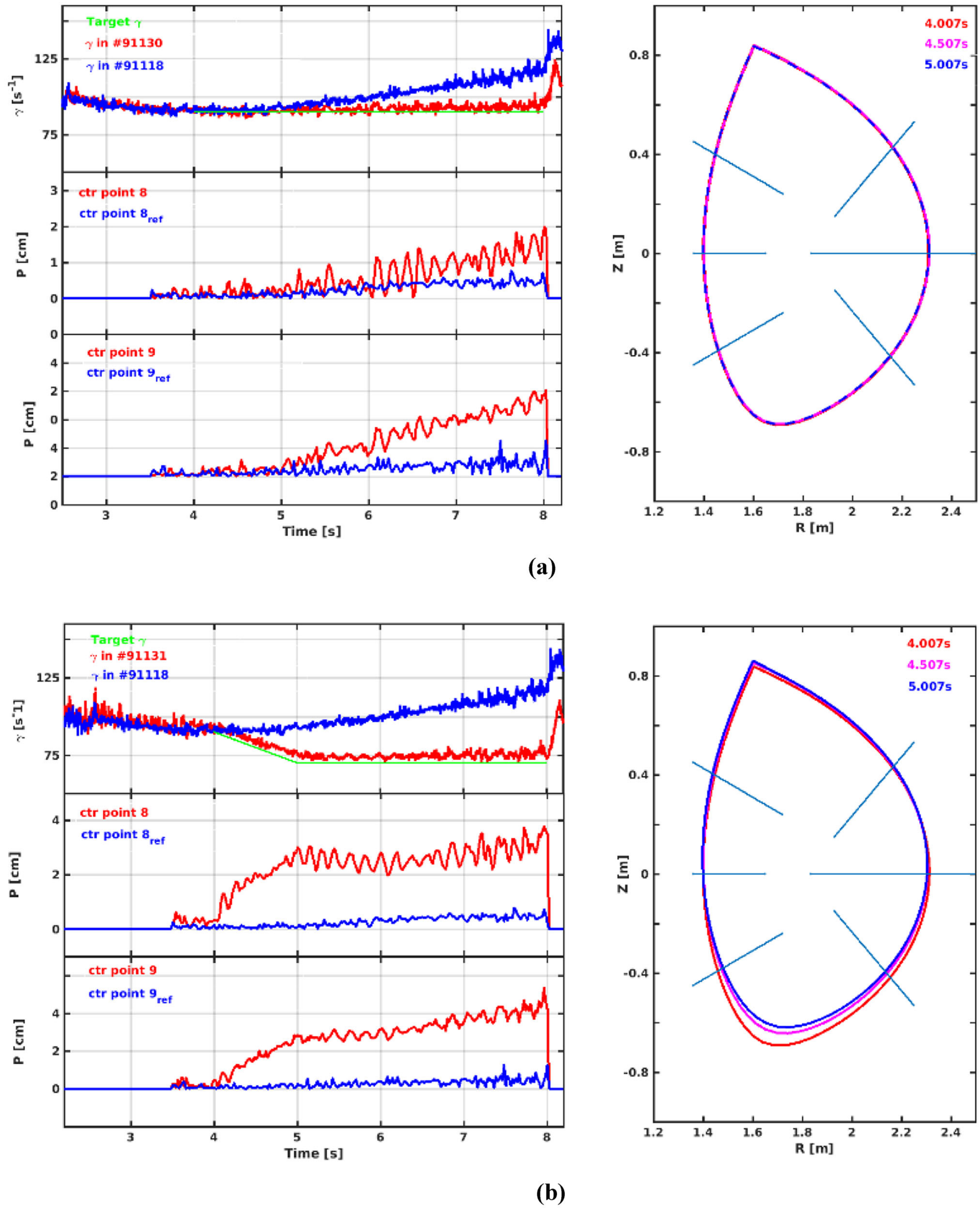

Fig. 6 (Color online) Results during EAST pulses #91130(**a**) and #91131(**b**), compared with those during the pulse #91118. The dark blue line represents evolution of plasma parameters in reference shot. The green and red lines represent target and real-time values. Plasma shapes at different times are shown in the right subfigures

6 Conclusion and discussion

In this study, feedback control of the vertical growth rate of plasma is designed and implemented on EAST. It includes three aspects: (1) the model-based vertical growth rate is calculated and integrated into the EAST PCS; (2) to continuously change the plasma shape with control point positions, a shape response model for gamma control is proposed based on history experiment analysis; (3) a gamma control algorithm is developed utilizing this shape response in the EAST PCS programming environment, which cooperates with ISOFLUX/PEFIT shape control. The EAST experiments demonstrate the gamma control's ability to ensure that the real-time vertical growth rate follows its corresponding target value. A gamma controller was developed to continuously keep the plasma away from inherent vertical instability to avoid plasma disruption, which is effective for tokamak plasma disruption prevention, especially for future large tokamak devices, such as ITER and CFETR, because catastrophic damage to plasma disruption is intolerable for these devices. More detailed design and experimental optimization for the gamma controller and its application to different plasma operation scenarios, such as double null (DN) and lower single null (LSN) configurations, need to be considered in future research.

Acknowledgements The authors would like to thank the members of the Institute of Plasma Physics Chinese Academy of Sciences (ASIPP) and the DIII-D team, especially all the researchers in the Department of Computer Application for their helpful discussions and support.

Author contributions All authors contributed to the study conception and design. Material preparation, data collection and analysis were performed by Na-Na Bao, Yao Huang, Bing-Jia Xiao, Qi-Ping Yuan, Zheng-Ping Luo, Yue-Hang Wang and Shu-Liang Chen. The first draft of the manuscript was written by Na-Na Bao and all authors commented on previous versions of the manuscript. All authors read and approved the final manuscript.

References

1. G. Tommasi, F. Maviglia, A.C. Neto et al., Plasma position and current control system enhancements for the JET ITER-like wall. Fusion Eng. Des. **89**, 233–242 (2014). https://doi.org/10.1016/j.fusengdes.2013.06.010
2. D.A. Humphreys, J.R. Ferron, A.W. Hyatt et al., DIII-D integrated plasma control solutions for ITER and next-generation tokamaks. Fusion Eng. Des. **83**, 193–198 (2008). https://doi.org/10.1016/j.fusengdes.2008.01.012
3. D. Mueller, S.H. Hahn, N. Eidietis et al., Improved fast vertical control in KSTAR. Fusion Eng. Des. **141**, 9–14 (2019). https://doi.org/10.1016/j.fusengdes.2019.02.046
4. Q.P. Yuan, B.J. Xiao, Z.P. Luo et al., Plasma current, position and shape feedback control on EAST. Nucl. Fusion **53**, 043009 (2013). https://doi.org/10.1088/0029-5515/53/4/043009
5. L. Liu, B.J. Xiao, D.A. Humphreys et al., Controllability study of EAST plasma vertical instability and improvement in future. Fusion Eng. Des. **89**, 563–567 (2014). https://doi.org/10.1016/j.fusengdes.2014.02.069
6. R. Albanese, R. Ambrosino, A. Castaldo et al., ITER-like vertical stabilization system for the east Tokamak. Nucl. Fusion **57**, 086039 (2017). https://doi.org/10.1088/1741-4326/aa7a78
7. G. Tommasi, B.J. Xiao, R. Albanese et al., Model-based plasma vertical stabilization and position control at EAST. Fusion Eng. Des. **129**, 152–157 (2018). https://doi.org/10.1016/j.fusengdes.2018.02.020
8. A. Hassanein, T. Sizyuk, M. Ulrickson, Vertical displacement events: a serious concern in future ITER operation. Fusion Eng. Des. **83**, 1020–1024 (2008). https://doi.org/10.1016/j.fusengdes.2008.05.032
9. T. Hender, J.C. Wesley, J. Bialek et al., Chapter 3: MHD stability, operational limits and disruptions. Nucl. Fusion **47**, S128 (2007). https://doi.org/10.1088/0029-5515/47/6/S03
10. D.A. Humphreys, T.A. Casper, N. Eidietis et al., Experimental vertical stability studies for ITER performance and design guidance. Nucl. Fusion **49**, 115003 (2009). https://doi.org/10.1088/0029-5515/49/11/115003
11. J.P. Qian, B.N. Wan, B. Shen et al., Vertical instability in EAST: comparison of model predictions with experimental results. Plasma Sci. Tech. **10**, 290–293 (2008). https://doi.org/10.1088/1009-0630/10/3/04
12. G. Ambrosino, M. Ariola, G. De Tommasi et al., Plasma vertical stabilization in the ITER tokamak via constrained static output feedback. IEEE T. Control Syst. Technol. **19**, 376–381 (2011). https://doi.org/10.1109/TCST.2010.2042601
13. Q.L. Qiu, B.J. Xiao, Y. Guo et al., Simulation of EAST vertical displacement events by Tokamak simulation code. Nucl. Fusion **56**, 106029 (2016). https://doi.org/10.1088/0029-5515/56/10/106029
14. Q.L. Qiu, Y. Guo, X. Gao et al., The numerical analysis of controllability of EAST plasma vertical position by TSC. Fusion Eng. Des. **141**, 116–120 (2019). https://doi.org/10.1016/j.fusengdes.2019.03.039
15. D.A. Humphreys, J.R. Ferron, M. Bakhtiari et al., Development of ITER-relevant plasma control solutions at DIII-D. Nucl. Fusion **47**, 943 (2018). https://doi.org/10.1088/0029-5515/47/8/028
16. N.N. Bao, Y. Huang, B.J. Xiao et al., A real-time disruption prediction tool for VDE on EAST. IEEE T. Plasma Sci. **48**, 715–720 (2020). https://doi.org/10.1109/TPS.2020.2972579
17. N.N. Bao, Y. Huang, J. Barr et al., Tests of the real-time vertical growth rate calculation on EAST. Chin. Phys. B **29**, 065204 (2020). https://doi.org/10.1088/1674-1056/ab84da
18. S.L. Chen, F. Villone, B.J. Xiao et al., Equivalent axisymmetric plasma response models of EAST. Plasma Phys. Control. Fusion **58**, 025017 (2016). https://doi.org/10.1088/0741-3335/58/2/025017
19. S.L. Chen, F. Villone, L. Barbato et al., Effect of three-dimensional conducting structures on vertical stability in EAST. Nucl. Fusion **55**, 013010 (2014). https://doi.org/10.1088/0029-5515/55/1/013010
20. S.L. Chen, F. Villone, Y.W. Sun et al., Comparison of different linearized plasma response models on the EAST tokamak. Nucl. Fusion **58**, 076009 (2018). https://doi.org/10.1088/1741-4326/aabe95
21. X.N. Yue, B.J. Xiao, Z.P. Luo et al., Fast equilibrium reconstruction for Tokamak discharge control based on GPU. Plasma Phys. Control. Fusion **55**, 085016 (2013). https://doi.org/10.1088/0741-3335/55/8/085016
22. Y. Huang, B.J. Xiao, Z.P. Luo et al., Implementation of GPU parallel equilibrium reconstruction for plasma control in EAST.

Fusion Eng. Des. **112**, 1019–1024 (2016). https://doi.org/10.1016/j.fusengdes.2016.02.048
23. Y. Huang, B.J. Xiao, Z.P. Luo, Fast parallel Grad-Shafranov solver for real-time equilibrium reconstruction in EAST tokamak using graphic processing unit. Chinese Phys. B **26**, 085204 (2017). https://doi.org/10.1088/1674-1056/26/8/085204
24. Y. Huang, Z.P. Luo, B.J. Xiao et al., GPU-optimized fast plasma equilibrium reconstruction in fine grids for real-time control and data analysis. Nucl. Fusion **60**, 076023 (2020). https://doi.org/10.1088/1741-4326/ab91f8
25. B.J. Xiao, Q.P. Yuan, Z.P. Luo et al., Enhancement of EAST plasma control capabilities. Fusion Eng. Des. **112**, 660–666 (2016). https://doi.org/10.1016/j.fusengdes.2016.06.004
26. B.J. Xiao, D.A. Humphreys, M.L. Walker et al., EAST plasma control system. Fusion Eng. Des. **83**, 181–187 (2008). https://doi.org/10.1016/j.fusengdes.2007.12.028
27. M.L. Walker, J.R. Ferron, D.A. Humphreys et al., Next-generation plasma control in the DIII-D tokamak. Fusion Eng. Des. **66–68**, 749–753 (2003). https://doi.org/10.1016/S0920-3796(03)00295-3
28. B.G. Penaflor, J.R. Ferron, M.L. Walker et al., Worldwide collaborative efforts in plasma control software development. Fusion Eng. Des. **83**, 176–180 (2008). https://doi.org/10.1016/j.fusengdes.2007.11.012
29. D.A. Gates, J.R. Ferron, M. Bell et al., Plasma shape control on the National Spherical Torus Experiment (NSTX) using real-time equilibrium reconstruction. Nucl. Fusion **46**, 17 (2005). https://doi.org/10.1088/0029-5515/46/1/002